Chemical Physics Letters 478 (2009) 230–233

Contents lists available at ScienceDirect

Chemical Physics Letters

journal homepage: www.elsevier.com/locate/cplett

High tensile modulus of carbon nanotube nano-fibers produced by dielectrophoresis

Han Zhang [a], Jie Tang [a], Pinwen Zhu [a], Jun Ma [a], Lu-Chang Qin [b,c,*]

[a] 1D Nanomaterials Research Group, National Institute for Materials Science, Sengen 1-2-1, Tsukuba, Ibaraki 305-0047, Japan
[b] W.M. Keck Laboratory for Atomic Imaging and Manipulation, Department of Physics and Astronomy, University of North Carolina at Chapel Hill, Chapel Hill, NC 27599-3255, USA
[c] Curriculum in Applied Sciences and Engineering, University of North Carolina at Chapel Hill, Chapel Hill, NC 27599-3255, USA

ARTICLE INFO

Article history:
Received 26 March 2009
In final form 28 July 2009
Available online 6 August 2009

ABSTRACT

We report an experimental measurement of the high tensile modulus of single-walled carbon nanotube (SWNT) bundles and SWNT nano-fibers produced by dielectrophoresis. The average tensile modulus of the SWNT nano-fibers is 265 GPa, much higher than the carbon nanotube fibers spun by other techniques. The tensile modulus increases as the diameter of the fiber decreases due to changes in the dielectrophoretic forces that densify the packing of SWNT bundles. Tensile modulus of 643 ± 86 GPa and 443 ± 14 GPa were obtained, respectively, from a SWNT bundle of 10 nm diameter and a SWNT nano-fiber of diameter 55 nm with a packing density of 69%, respectively.

1. Introduction

Carbon nanotubes (CNTs) are light and stiff with Young's modulus of about 1 TPa and tensile strength greater than 100 GPa as predicted by quantum mechanics calculations [1–3]. Experimental measurements of the mechanical properties including the strength of individual multiwalled carbon nanotubes (MWNTs) have demonstrated that the values approach theoretical predictions [4–6]. On the other hand, single-walled carbon nanotubes (SWNTs) tend to form bundles [7–9]. Practically, many applications involving single-walled carbon nanotubes actually use bundles instead of individuals and understanding of the mechanical properties of single-walled carbon nanotube bundles is of great interest to both scientific studies and industrial applications [10,11]. For example, carbon nanotubes (CNTs), especially single-walled carbon nanotubes, have been used as fillers to fabricate polymer composites or are woven directly into functional sheets with enhanced mechanical, electrical, and thermal properties [12–14].

To produce a carbon nanotube nano-fiber, one method is to assemble individual SWNTs or SWNT bundles in a head-to-tail manner. Unlike the covalent bonds within a SWNT, the bonding between SWNTs is largely through van der Waals forces, the strength of which also depends on the interfacial area and the packing density of the SWNTs. There have been two major methods reported in the literature for fabricating continuous long SWNT nano-fibers: (a) dry spin and (b) wet spin [15–18]. In both methods, the densification of SWNT bundles inside an SWNT nano-fiber is achieved by mechanical twisting, capillary pinching from the liquid medium, polymer binding, or a combination of all. However, the highest tensile modulus reported in the literature for the SWNT nano-fibers, 80 GPa, is still more than one order of magnitude lower than that of individual SWNTs. An alternative way of producing SWNT nano-fibers with a controllable diameter and length is dielectrophoresis [19], in which the dielectrophoretic forces also densify the as-drawn SWNT nano-fiber in addition to the capillary pinching forces provided by the liquid-fiber interfacial meniscus. Therefore, a dielectrophoretically drawn SWNT nano-fiber promises an even higher packing density as well as higher mechanical toughness and strength. On the other hand, SWNT nano-fibers of small diameter are also highly desirable in practical applications. For example, when they are used as fillers in composite materials, they would provide better load transfers because they have higher surface/volume ratios. The SWNT nano-fibers made by dielectrophoresis have also exhibited excellent mechanical rigidity, strength, and abrasion resistance when they are used as the atomic force microscope (AFM) probes [20]. Superb performance in field-induced electron emission has also been demonstrated using these single SWNT nano-fibers [21].

2. Experimental

The starting SWNT material was purchased commercially (Cheap Tubes, Inc.) and it was first examined in a transmission electron microscope (JEM-2010F) to reveal the structure and morphology of the SWNTs and SWNT bundles. The pristine SWNTs were then purified and cut to segments of length about 2 μm. The CNT–water suspension is prepared by dispersing the processed SWNTs in de-ionized water.

The SWNT nano-fibers of various lengths were then prepared using the dielectrophorestic method described in a previous publication [19]. A sharp tungsten needle, prepared by chemical etching,

* Corresponding author. Address: W.M. Keck Laboratory for Atomic Imaging and Manipulation, Department of Physics and Astronomy, University of North Carolina at Chapel Hill, Chapel Hill, NC 27599-3255, USA. Fax: +1 919 962 0480.
E-mail address: lcqin@physics.unc.edu (L.-C. Qin).

0009-2614/$ - see front matter © 2009 Published by Elsevier B.V.
doi:10.1016/j.cplett.2009.07.091

was used as the working electrode and a small metal ring was used as the counter electrode in the experimental set-up. The diameter of the SWNT nano-fibers is controlled to be from a few nanometers to a few microns by adjusting the processing parameters such as the concentration of SWNTs in the CNT–water suspension, the retrieving speed of the SWNT fiber from the CNT–water suspension, the applied AC voltage, and the frequency that are used in the dielectrophoretic drawing process.

For measurement of the mechanical properties of the dielectrophoretically produced SWNT fibers, a silicon substrate with nano-trenches was fabricated by growing a layer of SiO_2 onto the silicon wafer which had been masked by designed patterns drawn by photolithography. The nano-trenches, which are from 1.5 μm to 3 μm in width and 400 nm in depth, were fabricated on the final substrate. A drawn SWNT nano-fiber was then brought into contact with the substrate using a micromanipulator. The SWNT nano-fiber sticks firmly to the SiO_2 surface through van der Waals interactions. The finished SWNT nano-fiber nano-bridges were examined in a scanning electron microscope (SEM). To provide extra anchoring forces to prevent slippage between the SWNT nano-fiber and the SiO_2 substrate, a focused ion beam system (FIB) was also employed to deposit a layer of tungsten onto the SWNT nano-fiber. Both the fixed and unfixed structures were used to measure the elastic properties of the SWNT nano-fibers.

An atomic force microscope (AFM) was used for both imaging and performing force measurements on the SWNT nano-fiber nano-bridges. In order to prevent slippage between the AFM probe and the SWNT nano-fiber during vertical loading, we used a flattened AFM probe with a tip diameter of about 100 nm in the force measurements [22]. In the experiment, the AFM probe was loaded vertically on the desired positions with the force measured by detecting the amount of cantilever deflection while the sample displacement is recorded simultaneously [23]. In this study, the force–displacement curves were collected at three different locations on the substrate: (i) the mid-span of the nano-bridge, (ii) a segment of the SWNT nano-fiber sitting on the top of the trench, and (iii) the top surface of the substrate.

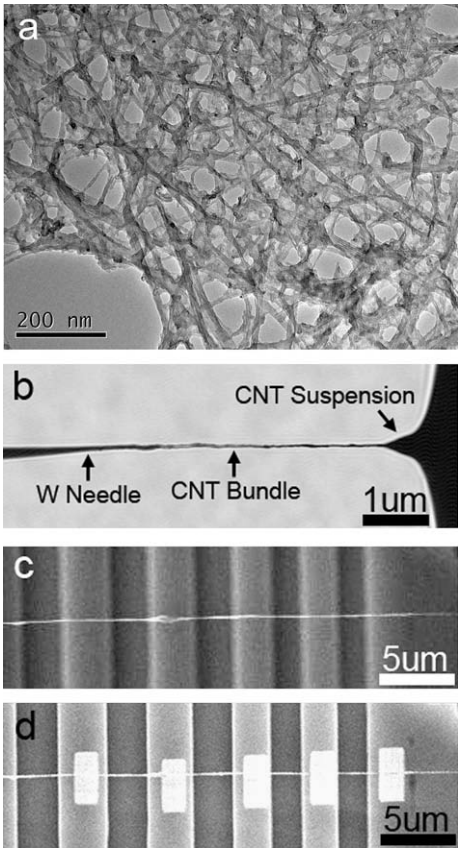

Fig. 1. (a) TEM image of the pristine SWNT material showing the SWNT bundles; (b) a SWNT nano-fiber is being drawn out of the SWNT suspension by a tungsten needle; (c) a SWNT nano-fiber laid on top of SiO_2 trenches forming five nano-bridges; (d) the same nano-bridge structure after being fixed to the substrate by deposition of tungsten using FIB.

3. Results and discussion

Fig. 1a shows the morphology of the pristine SWNT material observed with a transmission electron microscope (TEM). Individual SWNTs are found to agglomerate into bundles with an average diameter of 10 nm. A snapshot of the dielectrophoretic drawing in action is given in Fig. 1b, where a continuous SWNT nano-fiber is being produced. Fig. 1c is an SEM image of a SWNT nano-fiber lying on the nano-trenches fabricated on a silicon substrate with width between 1.5 μm and 3 μm and depth of about 400 nm. Fig. 1d shows the same structure depicted in Fig. 1c after tungsten pads were deposited using FIB to hold the SWNT nano-fiber in place.

Fig. 2a shows an AFM topographic image of the nano-bridge. Before the force measurements, the diameter of the SWNT nano-fiber was measured in the SEM, which is 66 nm, as shown in the inset of Fig. 2a. The three force–displacement curves obtained are displayed in Fig. 2b in the same colors (pink,[1] blue, and yellow) and marked with the same letters A, B, and C as the corresponding arrows and letters indicating their respective locations given in Fig. 2a. As shown in the figure, position A (pink) is on the bare substrate, position B (blue) is on the SWNT fiber lying on substrate, and position C (yellow) is at the mid-span of the SWNT fiber. The pink curve, acquired from the bare substrate, exhibits a straight line and its slope K_i equals to the spring constant of the silicon cantilever, K_c, which is 0.78 N/m as calibrated by using a standard calibration cantilever [24]. The slope of the blue curve K_{ii}, acquired from a position on the SWNT fiber with solid support from the substrate underneath the SWNT fiber, represents a combination of spring constants of both the silicon cantilever, K_c, and the radial compressional spring constant of the SWNT nano-fiber, K_r, with a relationship

$$K_{ii} = \frac{K_c K_r}{K_c + K_r}. \quad (1)$$

The measured value of K_{ii} is 0.68 N/m. The total displacement recorded at the mid-span of the nano-bridge is due to the displacements from the cantilever, the radial compression of the SWNT nano-fiber, and the axial stretching of the SWNT nano-fiber. Therefore, the slope of the yellow curve, K_{iii}, acquired at position C, is a combination of all three corresponding spring constants, which can be expressed as

$$K_{iii} = \frac{K_{ii} K_t}{K_{ii} + K_t} = 0.60\ \mathrm{N/m}, \quad (2)$$

where

$$K_t = \frac{K_{ii} K_{iii}}{K_{ii} - K_{iii}} \quad (3)$$

is the tensile spring constant of the SWNT nano-fiber. It is revealed in the graph that both the blue curve B and the yellow curve C begin to deviate from straight lines after a region of low displacement. It indicates the elastic limit and the starting of plastic deformation in

[1] For interpretation of color in Figs. 2 and 3, the reader is referred to the web version of this article.

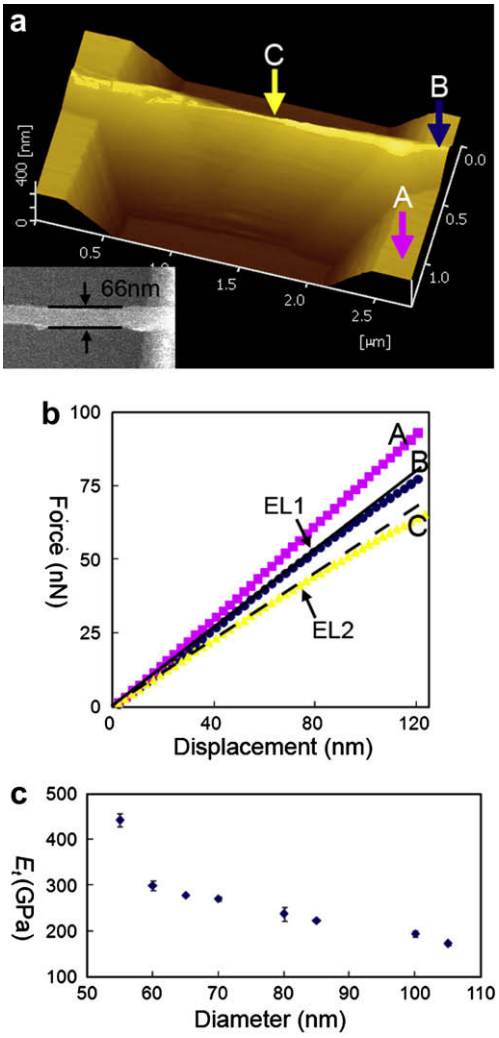

Fig. 2. (a) AFM topographic image of a SWNT nano-fiber nano-bridge with the inset being an SEM image of its suspended section; (b) force–displacement curves obtained by loading vertically the AFM probe on the three positions indicated by colored arrows (letters) in (a); (c) tensile modulus obtained from eight SWNT nano-fibers of different diameters.

the radial compression and/or axial stretching. The positions of elastic limit are labeled as EL1 and EL2 in the graph [25]. In this study, the tensile modulus E_t of the SWNT nano-fiber is evaluated using the classical model of three-point bending on a clamped beam. E_t is calculated from the experimentally measured tensile spring constant, K_t, of the SWNT nano-fiber by

$$E_t = \frac{K_t L^3}{192I}, \tag{4}$$

where L is the span length of the nano-bridge and I is the moment of inertia of the SWNT nano-fiber cross section, which can be calculated by $I = \pi r^4/4$ with r being the radius of the SWNT nano-fiber [25]. For the SWNT nano-fiber shown in Fig. 2, $L = 2.17$ μm and $r = 33$ nm. As a result, an average tensile modulus of $E_t = 293$ GPa was obtained over two consecutive measurements for this SWNT nano-fiber.

The same procedure was used to obtain E_t for another seven SWNT nano-fibers with different diameters in the present study. The tensile modulus E_t shows a clear descending trend as the SWNT nano-fiber diameter increases. The tensile moduli of the eight SWNT nano-fibers tested are plotted in Fig. 2c with respect to their diameter. E_t decreased significantly from 443 GPa to 173 GPa as the diameter of the SWNT nano-fiber increased from 50 nm to 100 nm. The same measurement procedure was also performed after the SWNT nano-fiber was fixed by depositing tungsten pads on top of the SWNT nano-fiber across each trench. However, consistent values of modulus were obtained and this indicates that the anchoring forces provided by the frictions between the SWNT nano-fiber and the SiO_2 substrate are sufficient to prevent slippage during force loading.

To correlate the mechanical properties of the SWNT nano-fibers with the dielectrophoretic drawing process, another experiment was performed to measure the elastic moduli of the constituting individual SWNT bundles. Electron beam lithography was used this time to fabricate a platform structure on a silicon substrate with square pits of 250 nm in width and 200 nm in depth. The SWNT–water suspension used in the previous experiment was then spin-coated onto the substrate surface. Several SWNT bundles of about 10 nm in diameter happened to be running across some pits to form nano-bridges. An AFM image of one such nano-bridge is shown in Fig. 3a. The dimensions of the SWNT bundle are measured in the SEM and they are labeled in the inset of the figure. The three arrows, colored in blue (A), pink (B), and yellow (C), indicate the three locations (A, B, and C) selected for the force–displacement measurements: (A) the solid substrate surface, (B) a

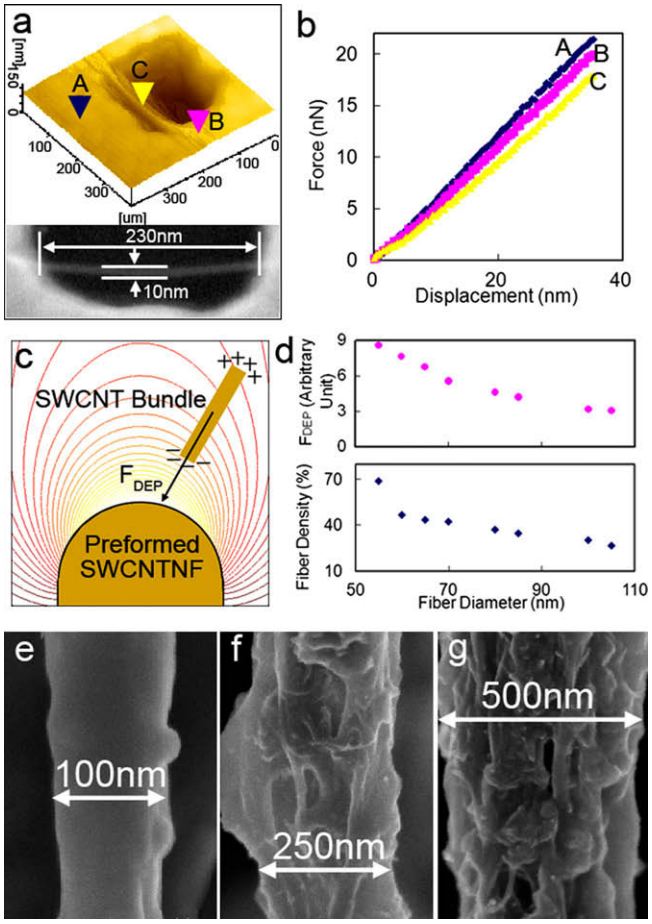

Fig. 3. (a) AFM topographic image of a nano-bridge structure formed by a SWNT bundle; the inset is an SEM image showing the dimensions of the bundle; (b) force–displacement curves obtained from the three positions indicated by colored arrows (letters) in (a); (c) simulation model of a SWNT bundle attracted by dielectrophoretic forces towards the tip of the preformed SWNT nano-fiber; (d) simulated dielectrophoretic forces and measured packing densities of eight SWNT nano-fibers plotted with respect to their diameter; (e–g) high-resolution SEM images showing different surface morphologies of the SWNT nano-fibers with increasing diameters as indicated in the respective diagrams.

segment of the SWNT bundle on the top surface of the substrate, and (C) the mid-span of the nano-bridge. The measured force–displacement curves are displayed in Fig. 3b with the same colors and letters as their corresponding arrows. Using Eqs. (2) and (3) and following the same calculations, we obtained the tensile modulus E_t of the SWNT bundle with a average of 643 ± 86 GPa over five consecutive measurements.

Since the SWNT nano-fibers are composed of mostly SWNT bundles, by assuming voids and the SWNT bundles of 10 nm in diameter are the only two elements in the entire SWNT nano-fiber, we applied the law of mixture, $E_{fiber} = \nu E_{bundle}$, to estimate the volume density ν of the SWNT bundles inside a SWNT nano-fiber after knowing the respective moduli of the fiber E_{fiber} and the bundle E_{bundle}, respectively. For the SWNT nano-fiber characterized in Fig. 2a, $\nu = 43.5\%$ was obtained.

Fig. 3c illustrates the dielectrophoretic forces that the SWNT bundle is subject to with an electric field being applied between the preformed SWNT nano-fiber and the holder ring in the suspension. The SWNT bundle is aligned and attracted by the dielectrophoretic forces towards the gradient of the electric field strength squared, $F_{DEP} = C\nabla E^2$, where C is a constant related to the AC field frequency, geometry of the SWNT bundle, dielectric constants and conductivities of the medium (water), and the SWNT bundle [26]. The dielectrophoretic forces attract the nearby SWNT bundles towards each other and pack them into the preformed SWNT nano-fiber. As the diameter of the preformed SWNT nano-fiber changes, the electric field distribution also changes in the suspension, resulting in a change in the dielectrophoretic forces and the packing density of the newly added SWNT bundles. We have calculated ∇E^2 in the vicinity of the preformed SWNT nano-fiber tip using computer simulations (FEBLAB) for each SWNT nano-fiber diameter encountered in the elastic modulus measurement. The F_{DEP} values are obtained by assigning an arbitrary value for the coefficient C and are plotted against each diameter in the top portion of Fig. 3d. The packing densities calculated from the tensile modulus are also plotted with respect to each diameter at the bottom portion of the figure. Both plots show a decrease in value with increasing SWNT nano-fiber diameters. There are two types of forces that tend to densify the packing of SWNT bundles inside a SWNT nano-fiber during the dielectrophoretic drawing process: (i) the capillary forces at the interfacial meniscus and (ii) the dielectrophoretic forces inside the suspension. Since the capillary forces are determined only by surface tensions of the contacting interfaces, it should be independent of the SWNT nano-fiber diameter. Therefore, the decrease in dielectrophoretic forces should account for the decrease in packing density of the SWNT nano-fibers as their diameter increases. To further clarify the above mechanism, we also used a high-resolution SEM to examine the morphology of three SWNT nano-fibers with diameters of 100 nm, 250 nm and 500 nm, respectively. It is clearly shown in Fig. 3e–g that, as the diameter of the fiber increases, the original smooth surface (Fig. 3e) of the SWNT nano-fiber changes into a rough surface (Fig. 3f), and eventually distributed with visible holes (Fig. 3g). The cross section of a SWNT nano-fiber has a density gradient from a densely packed core to a loosely packed outer shell because the dielectrophoretic forces exerted on the SWNT bundles decrease as the SWNT nano-fiber grows thicker.

The measured tensile modulus for the SWNT bundle, 643 ± 86 GPa, is within the range of theoretical predictions and it shows good reliability of the method used in this study. The tensile modulus of the SWNT nano-fiber is 265 GPa averaged over the eight SWNT nano-fibers tested in the experiment. This value is more than three times larger than the stiffest continuous CNT-fiber reported in the literature [24]. The dependence of the SWNT nano-fiber packing density on dielectrophoretic forces makes it possible now to achieve even higher tensile strength and stiffness. In addition, dielectrophoretic spinning is a unique method that is capable of producing continuous CNT-fibers of very small diameter.

4. Conclusions

Single-walled carbon nanotube nano-fibers produced by dielectrophoresis exhibit high tensile modulus with an average of 265 GPa. The tensile modulus increases as the diameter of the carbon nanotube nano-fiber decreases. The highest tensile modulus of about 650 GPa has been measured from a single-walled carbon nanotube bundle of 10 nm in diameter.

Acknowledgements

We wish to thank financial support from the JSPS Grants-in-Aid for Scientific Research No. 19710101, the Shorai Foundation for Science and Technology, and the 'Nanotechnology Network Project' of the Ministry of Education, Culture, Sports, Science and Technology (MEXT), Japan.

References

[1] J.P. Lu, Phys. Rev. Lett. 79 (1997) 1297.
[2] S. Ogata, Y. Shibutani, Phys. Rev. B 68 (2003) 165409.
[3] G.G. Samsonidze, G.G. Samsonidze, B.I. Yakobson, Phys. Rev. Lett. 88 (2002) 065501.
[4] M.M.J. Treacy, T.W. Ebbesen, J.M. Gibson, Nature 381 (1996) 678.
[5] M.-F. Yu, O. Lourie, M.J. Dyer, K. Moloni, T.F. Kelly, R.S. Ruoff, Science 287 (2000) 637.
[6] B. Peng, M. Locascio, P. Zapol, S. Li, S.L. Mielke, G.C. Schatz, H.D. Espinosa, Nat. Nanotechnol. 3 (2008) 626.
[7] A. Thess et al., Science 273 (1996) 483.
[8] L.-C. Qin, S. Iijima, H. Kataura, Y. Maniwa, S. Suzuki, Y. Achiba, Chem. Phys. Lett. 268 (1997) 101.
[9] L.-C. Qin, S. Iijima, Chem. Phys. Lett. 269 (1997) 65.
[10] D.A. Walters, L.M. Ericson, M.J. Casavant, J. Liu, D.T. Colbert, K.A. Smith, R.E. Smalley, Appl. Phys. Lett. 74 (1999) 3803.
[11] M.-F. Yu, B.S. Bradley, S. Arepalli, R.S. Ruoff, Phys. Rev. Lett. 84 (2000) 5552.
[12] M. Moniruzzaman, K.I. Winey, Macromolecules 39 (2006) 5194.
[13] A.B. Dalton et al., Nature 423 (2003) 703.
[14] M. Zhang et al., Science 309 (2005) 1215.
[15] X. Zhang et al., Adv. Mater. 18 (2006) 1505.
[16] H.W. Zhu, C.L. Xu, D.H. Wu, B.Q. Wei, R. Vajtai, P.M. Ajayan, Science 296 (2002) 884.
[17] M. Zhang, K.R. Atkinson, R.H. Baughman, Science 306 (2004) 1358.
[18] B. Vigolo, P. Poulin, M. Lucas, P. Launois, P. Bernier, Appl. Phys. Lett. 81 (2002) 1210.
[19] J. Tang, B. Gao, H. Geng, O.D. Velev, L.-C. Qin, O. Zhou, Adv. Mater. 15 (2003) 1352.
[20] J. Tang et al., Nano Lett. 5 (2005) 11.
[21] J. Zhang, J. Tang, G. Yang, Q. Qiu, L.-C. Qin, O. Zhou, Adv. Mater. 16 (2004) 1219.
[22] H. Zhang, J. Tang, L. Zhang, B. An, L.-C. Qin, Appl. Phys. Lett. 92 (2008) 173121.
[23] J.P. Salvetat et al., Phys. Rev. Lett. 82 (1999) 944.
[24] M. Tortonese, M. Kirk, Proc. SPIE 3009 (1997) 53.
[25] P.G. Laurson, W.J. Cox, Mechanics of Materials, John Wiley & Sons, Inc., New York, USA, 1954.
[26] T.B. Jones, Electromechanics of Particles, Cambridge University Press, Cambridge, UK, 1995.